#### RESEARCH



# Complex dynamics of Mandelbrot sets induced by iterative composition of two polynomials under the Das-Debata framework

Subhadip Roy<sup>1</sup> · Krzysztof Gdawiec<sup>2</sup>

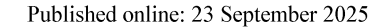
Received: 16 June 2025 / Accepted: 26 August 2025 © The Author(s) 2025

#### Abstract

Research on the Mandelbrot set has been ongoing for decades and occupies a significant place in the study of fractal geometry. It is obtained by employing a function in the complex plane in an iterative procedure. This method is further developed in existing literature in two ways: either by employing complicated functions of various kinds or by using iterative methods beyond the standard Picard iteration. In both cases, we use a single function to obtain the Mandelbrot set. In this paper, we propose an approach in which we use two polynomial functions instead of one. For this aim, we have utilized the Das-Debata iteration, which combines two operators into a single iterative process. Polynomials of the form  $z^m + pz + r$ , where  $z, p, r \in \mathbb{C}$ ,  $m \in \mathbb{N}$ , and m > 2, are used to derive the escape criterion. By employing the escape time algorithm, we have provided interesting graphical representations of Mandelbrot sets that exhibit notable variations in patterns compared to those obtained by the Picard iteration. To create a comparison analysis of the resulting sets based on the iteration parameters, we merged polynomials of the same degree and different degrees and changed their ordering in the iterative process. Finally, we examined two numerical measures: the average escape time and the non-escaping area index, to determine how these fractal sets rely on the iteration parameters, which turns out that the dependency of both iterative approaches is nonlinear

**Keywords** Escape criteria · fractal · Mandelbrot set · Das–Debata iteration

Extended author information available on the last page of the article





## 1 Introduction

Fractal geometry offers a foundation for analyzing complex, self-similar patterns that appear in mathematical systems and in nature [21]. The Mandelbrot set is one of the most celebrated fractals and its boundary reveals an infinite complexity governed by a simple iterative method, making it a rich subject of exploration in both theoretical and applied contexts. A popular method for generating fractals is through the successive iterative method

$$z_{k+1} = f(z_k), \tag{1}$$

where *f* is a well-defined complex function. This method has wide applications in generating fractals of different varieties, such as the Mandelbrot set [21], the Julia set [9], Biomorphs [18], root-finding fractals [11, 14] (the so-called polynomiography), iterated function system [6], inversion fractals [22] etc.

Our focus in this paper is only on the Mandelbrot set, which is defined using the feedback process (1) and the quadratic complex polynomial  $f_c(z) = z^2 + c$ , where c is a complex number. Many generalizations of the Mandelbrot set have now been developed by researchers. Lakhtakia et al. suggested utilizing polynomials of the type  $z^p + c$  instead of the quadratic one in [19]. Several studies have used the rational function, including [7, 25]. Works like [10, 15] have used functions, including exponential and trigonometric kinds. The initial development of the Mandelbrot and the Julia set is based on the iterative process (1), which is famously known as the Picard iteration. In the context of fractal generation, Rani and Kumar in [24] utilized the Mann iteration process, a generalization of the Picard iteration, to produce superior Julia sets for the first time in 2004. A two-step Ishikawa iteration process for the relative superior Julia and Mandelbrot sets was examined by Rana et al. in [23]. In [4], a three-step Noor iteration method was employed to produce Mandelbrot and Julia sets. The viscosity iteration method is applied in [16, 18] for generating fractals from polynomial functions. Hybrid iteration methods such as Picard–Mann, Picard—S, and Picard—Thakur have been utilized to produce Mandelbrot and Julia sets in works like [2, 27, 31]. Another development in this direction is due to Tanveer et al. [29], where the authors replaced the parameter c of the function  $z^p + c$  by  $\log c^t$  and used the Mann and Picard–Mann iteration to generate Mandelbrot sets. Subsequently, this function was used to create fractals through CR iteration [28] and four-step iteration [1]. In addition to the explicit iterations, various implicit iterations such as Jungck-Mann [20], Jungck-Ishikawa [3], and Jungck-Noor [30] have contributed to the generation of fractals.

In the extensive body of research on fractal generation—particularly for Mandelbrot and Julia sets—most studies have concentrated on the dynamics of a single complex function under fixed-point iteration. Comparatively little attention has been given to combining multiple functions within this framework. The only notable approach in this direction has been the Das—Debata iteration, a generalization of the Ishikawa iteration originally developed for studying common fixed points of quasi-nonexpansive mappings. In [11], this iteration was applied to two root-finding methods, producing fractal images that reflected the combined



dynamics of the methods. Later, in [26], the same iteration was employed to generate Mandelbrot and Julia sets corresponding to a polynomial and a rational function.

In this paper, we advance this line of work by, for the first time in the literature, applying the Das–Debata iteration to a pair of polynomials, thereby extending the approach of [26]. Specifically, we establish an escape criterion for polynomials of the form  $z^m + pz + r$  and present graphical examples of Mandelbrot sets arising from combinations of two polynomials, both of equal and differing degrees, with their placement within the iteration scheme systematically varied. Furthermore, to explore how the fractal structures depend on iteration parameters, we employ two numerical measures—the average escape time and the non-escaping area index—introduced in [17].

The structure of the rest of the paper is as follows. Some prerequisites necessary for the rest of the paper are presented in Section 2. In Section 3, we establish the escape criterion for the functions and iteration scheme under consideration. Section 4 includes some graphical examples of Mandelbrot sets and their comparison. In Section 5, we examine the relationships between the parameters of the iteration and the numerical measures. In Section 6, we provide some final remarks.

## 2 Preliminaries

We introduce the essential definitions in this section to lay the groundwork for our main result.

**Definition 1** ([9]) Let  $T_c$  be a complex function with a complex parameter c. The filled Julia set of  $T_c$  is defined as

$$\mathscr{F}_{T_c} = \{ z \in \mathbb{C} : |T_c^n(z)| \nrightarrow \infty \text{ as } n \to \infty \}.$$

The boundary of the filled Julia set  $\mathscr{F}_{T_c}$  is called a Julia set  $\mathscr{J}_{T_c}$ , i.e.,  $\mathscr{J}_{T_c} = \partial \mathscr{F}_{T_c}$ .

**Definition 2** ([32]) The Mandelbrot set for a complex function  $T_c$ , where c is a complex parameter, is defined as the set of parameters  $c \in \mathbb{C}$  for which  $\mathscr{J}_{T_c}$  is connected. Equivalently, the Mandelbrot set can be defined as

$$\mathscr{M} = \{c \in \mathbb{C} : |T^n_c(\eta)| \nrightarrow \infty \text{ as } n \to \infty\},$$

where  $\eta$  is a critical point of  $T_c$ , i.e.,  $T'_c(\eta) = 0$ .

**Definition 3** ([13]) Let  $T: X \to X$  be a mapping and  $\{z_n\}$  be a sequence in a space X (e.g., the complex numbers space) with an initial  $z_0 \in X$ . Then, the sequence is called the Ishikawa iteration if

$$x_k = (1 - \alpha_k)z_k + \alpha_k T(z_k), z_{k+1} = (1 - \beta_k)z_k + \beta_k T(x_k),$$
(2)



where  $\{\alpha_k\}, \{\beta_k\}$  are sequences in (0, 1].

Das and Debata generalized the Ishikawa iteration for two operators  $T, S: X \to X$  and applied it to find common fixed points of quasi-nonexpansive mappings [8].

**Definition 4** ([8]) Let  $S, T : X \to X$  be mappings and  $\{z_n\}$  be a sequence in a space X (e.g., the complex numbers space) with an initial  $z_0 \in X$ . Then, the sequence is called the Das-Debata iteration if

$$x_k = (1 - \alpha_k)z_k + \alpha_k S(z_k), z_{k+1} = (1 - \beta_k)z_k + \beta_k T(x_k),$$
(3)

where  $\{\alpha_k\}, \{\beta_k\}$  are sequences in (0, 1].

Let us notice that the iteration (3) with S = T reduces to the Ishikawa iteration.

In the rest of the paper, we assume that  $\{\alpha_k\}$ ,  $\{\beta_k\}$  are the constant sequences  $\alpha_k = \alpha$ ,  $\beta_k = \beta$ , where  $\alpha, \beta \in (0, 1]$ .

## 3 Escape criteria

In this section, we employ the Das-Debata iteration scheme (3) in conjunction with two complex polynomials to establish the escape criterion necessary for developing escape time algorithm used in generating Mandelbrot sets.

**Theorem 1** Let  $T_r(z) = z^m + pz + r$  and  $S_r(z) = z^n + qz + r$ , where  $m, n \in \mathbb{N} \setminus \{1\}$ , and  $p, q, r \in \mathbb{C}$ . Moreover, let  $\{z_k\}$  be the Das-Debata orbit of  $z_0 \in \mathbb{C}$ , i.e.,

$$x_k = (1 - \alpha)z_k + \alpha S_r(z_k),$$
  

$$z_{k+1} = (1 - \beta)z_k + \beta T_r(x_k),$$
(4)

where,  $\alpha, \beta \in (0, 1]$ . Suppose that

$$|z_0| > \max\left\{|r|, \left(\frac{2+\alpha|q|}{\alpha}\right)^{\frac{1}{n-1}}, \left(\frac{2+\beta|p|}{\beta}\right)^{\frac{1}{m-1}}\right\}.$$
 (5)

Then  $\lim_{k\to\infty} |z_k| = \infty$ .

**Proof** For k=0 in the first step of the Das–Debata iteration, we have

$$|x_0| = |(1-\alpha)z_0 + \alpha (z_0^n + qz_0 + r)| \\ \ge \alpha |z_0|^n - \alpha |qz_0| - \alpha |r| - (1-\alpha)|z_0|.$$
(6)

From (5), we have  $|z_0| > |r|$ . Therefore, from (6) we get



$$|x_{0}| \geq \alpha |z_{0}|^{n} - \alpha |qz_{0}| - \alpha |z_{0}| - (1 - \alpha)|z_{0}|$$

$$= \alpha |z_{0}|^{n} - \alpha |qz_{0}| - |z_{0}|$$

$$= |z_{0}|(\alpha |z_{0}|^{n-1} - \alpha |q| - 1).$$
(7)

Again from (5), we get  $|z_0| > \left(\frac{2+\alpha|q|}{\alpha}\right)^{\frac{1}{n-1}}$ . Which implies that

 $\alpha |z_0|^{n-1} - \alpha |q| - 1 > 1$ . Therefore, from (7), we have

$$|x_0| > |z_0|.$$
 (8)

Proceeding to the second step of the Das-Debata iteration, we have

$$|z_1| = |(1-\beta)z_0 + \beta(x_0^m + px_0 + r)| \ge \beta|x_0|^m - \beta|px_0| - \beta|r| - (1-\beta)|z_0|.$$
(9)

Using the condition  $|z_0| > |r|$ , we get

$$|z_1| \ge \beta |x_0|^m - \beta |px_0| - \beta |z_0| - (1 - \beta)|z_0| = \beta |x_0|^m - \beta |p||x_0| - |z_0|.$$
(10)

Since  $|x_0| > |z_0|$ , from (10), we get

$$|z_1| \ge \beta |x_0|^m - \beta |p| |x_0| - |x_0| = |x_0| (\beta |x_0|^{m-1} - \beta |p| - 1).$$
(11)

From (5) and (8), we have

$$|x_0| > |z_0| > \left(\frac{2+\beta|p|}{\beta}\right)^{\frac{1}{m-1}}.$$
 (12)

Therefore,  $\beta |x_0|^{m-1} - \beta |p| - 1 > 1$ . Thus, from (5) and (11), we get

$$|z_1| > |x_0| > |z_0|. (13)$$

Therefore, there exists some  $\gamma > 0$  such that  $|z_1| \ge (1+\gamma)|z_0|$ .

Because  $|z_1| > |z_0|$ , so we may repeat the same reasoning for k = 1 obtaining

$$|z_2| \ge (1+\gamma)|z_1| \ge (1+\gamma)^2|z_0|. \tag{14}$$

Therefore, at the k-th iteration, we get

$$|z_k| \ge (1+\gamma)^k |z_0|. (15)$$

Hence  $|z_k| \to \infty$  as  $k \to \infty$ .

From Theorem 1 we get the following corollary.



**Corollary 1** Let  $T_r(z) = z^m + pz + r$  and  $S_r(z) = z^n + qz + r$ , where  $m, n \in \mathbb{N} \setminus \{1\}$ , and  $p, q, r \in \mathbb{C}$ . Moreover, let  $\{z_k\}$  be the Das-Debata orbit of  $z_0 \in \mathbb{C}$ , i.e.,

$$x_k = (1 - \alpha)z_k + \alpha S_r(z_k), z_{k+1} = (1 - \beta)z_k + \beta T_r(x_k),$$
(16)

where,  $\alpha, \beta \in (0, 1]$ . Suppose that

$$|z_l| > \max\left\{|r|, \left(\frac{2+\alpha|q|}{\alpha}\right)^{\frac{1}{n-1}}, \left(\frac{2+\beta|p|}{\beta}\right)^{\frac{1}{m-1}}\right\},\tag{17}$$

for some  $l \in \mathbb{N}$ . Then  $\lim_{k \to \infty} |z_k| = \infty$ .

**Remark 1** For the sequence  $\{z_k\}$  defined in (4), the value

$$R = \max\left\{ |r|, \left(\frac{2+\alpha|q|}{\alpha}\right)^{\frac{1}{n-1}}, \left(\frac{2+\beta|p|}{\beta}\right)^{\frac{1}{m-1}} \right\}$$
 (18)

is called the escape radius.

## 4 Graphical examples of mandelbrot sets

In this section, we use the Das–Debata iteration which uses two polynomial functions to illustrate some graphical examples of Mandelbrot sets that are generated using the escape-time algorithm shown in Algorithm 1. The graphical examples of the Mandelbrot sets are generated by varying both the parameters  $\alpha$ ,  $\beta$  of the Das–Debata iteration as well as by changing the position of the two polynomials in the iteration process. Additionally, we apply both polynomials independently in the Picard iteration method to show the difference between those sets and the set obtained as a combination of both polynomials via the Das–Debata iteration.



**Input**:  $S_r$ ,  $T_r : \mathbb{C} \to \mathbb{C}$  – functions considered in Theorem 1;  $\alpha$ ,  $\beta \in (0, 1]$  – parameters for the Das–Debata iteration;  $A \subset \mathbb{C}$  – area; K – the maximum number of iterations; colormap[0..H] – color map with H+1 colors.

Output: Mandelbrot set for area A.

```
 \begin{array}{lll} \mathbf{1} & \mathbf{for} \ r \in A \ \mathbf{do} \\ \mathbf{2} & R = \max \left\{ |r|, \left( \frac{2+\alpha|q|}{\alpha} \right)^{\frac{1}{n-1}}, \left( \frac{2+\beta|p|}{\beta} \right)^{\frac{1}{m-1}} \right\} \\ \mathbf{3} & k = 0 \\ \mathbf{4} & z_0 = r \\ \mathbf{5} & \mathbf{while} \ |z_k| < R \ \mathbf{and} \ k < K \ \mathbf{do} \\ \mathbf{6} & x_k = (1-\alpha)z_k + \alpha S_r(z_k) \\ z_{k+1} = (1-\beta)z_k + \beta T_r(x_k) \\ k = k+1 \\ \mathbf{9} & i = \lfloor H \frac{K}{K} \rfloor \\ \mathbf{10} & \mathrm{color} \ r \ \mathrm{with} \ colormap[i] \\ \end{array}
```

#### Algorithm 1 Generation of Mandelbrot set.

In the first example, we consider  $A = [-2, 1] \times [-1.5, 1.5]$ , K = 50, the color map presented in Fig. 1, and the following functions:

$$F_1(z) = z^4 + r, (19)$$

$$F_2(z) = z^2 + r. (20)$$

In Fig. 2, we present examples of Mandelbrot sets generated using the Picard iteration for the complex polynomials  $F_1$  and  $F_2$ , respectively. Figure 2(b) depicts the classical Mandelbrot set for the 2nd-degree polynomial, while the set for the 4th-degree polynomial, shown in Fig. 2(a), exhibits a distinct 3-fold symmetry.

The combination of the  $F_1$  and  $F_2$  polynomials in the Das–Debata iteration produces unique patterns in the Mandelbrot sets, as illustrated in Figs. 3, 4, 5 and 6, which are dependent on the iteration parameters  $\alpha$ ,  $\beta$ . In Fig. 3 we fix the parameter  $\beta$  at 0.9 and vary the parameter  $\alpha$  with  $T=F_1$  and  $S=F_2$ . In Fig. 3(a), with  $\alpha=0.2$ , the Mandelbrot set exhibits symmetry about the x-axis and displays a more rounded shape. As  $\alpha$  increases, the sets retain their symmetry but shift toward the center of the region. Additionally, a slight reduction in the size of the sets is observed, and the budlike structures along the boundaries become more prominent. The Mandelbrot sets in Fig. 4 are generated using the same parameter values as in Fig. 3, but with different orders of the polynomials in the Das–Debata iteration, i.e.,  $T=F_2$  and  $S=F_1$ . The resulting Mandelbrot sets remain symmetric about the x-axis, but their overall structure differs significantly from those in Fig. 3. A sharp reduction in the size of the set is observed as  $\alpha$  increases from 0.2 to 0.6. Additionally, two small disconnected components appear at the top right and bottom corners of the region, which gradually move closer to the central body of the set as  $\alpha$  increases.

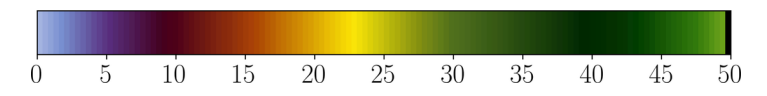


Fig. 1 Color map used in the graphical examples of Mandelbrot sets

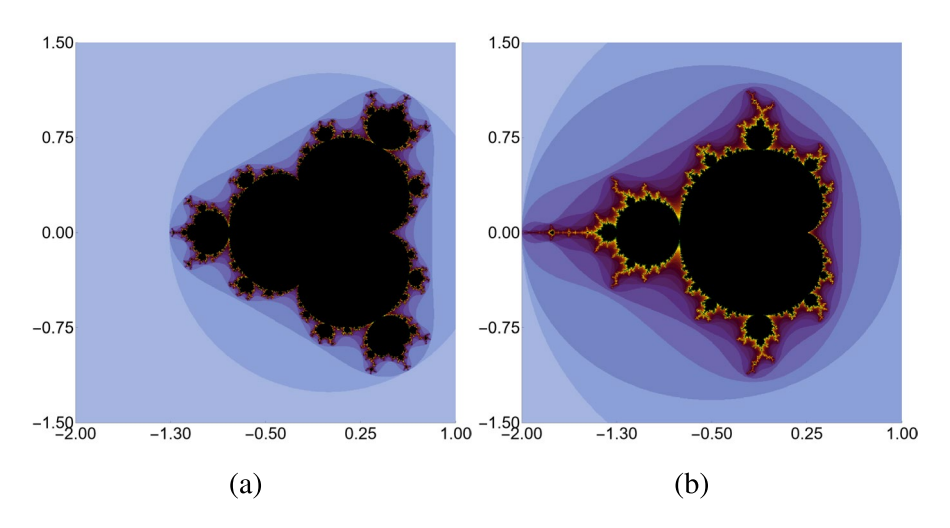


Fig. 2 Mandelbrot sets generated by Picard iteration with (a)  $F_1$  and (b)  $F_2$  functions

In Fig. 5, we have taken into account the variation in the parameter  $\beta$  and fixed value of  $\alpha = 0.01$  with  $T = F_1$ ,  $S = F_2$  in the Das–Debata iteration. The resultant Mandelbrot sets show a perfect 3-fold symmetry for all the considered values of the parameter  $\beta$ . This characteristic is mostly dominated by the 4th-degree polynomial  $z^4 + r$ , and it also happens when a 4th-degree polynomial is used in Picard iteration (Fig. 2(a)). The size of the sets reduces as the values of  $\beta$  are increased and this is mostly evident when  $\beta$  is increased from 0.2 to 0.6. Also, with the increasing values of  $\beta$ , the boundary of the set becomes more complex. Nearly resembling the Mandelbrot set generated for the 4th-degree polynomial with the Picard iteration, many bud-like components of varying sizes are visible on the boundary of the set for  $\beta = 1$ . With the same parameter values as in Fig. 5, and by changing the ordering of the polynomials, i.e.,  $T = F_2$  and  $S = F_1$ , Fig. 6 displays the resulting Mandelbrot sets. In this instance, we observe that the properties of the 2nd-degree polynomial mostly dominate the Mandelbrot sets. The majority of the region is covered in black for  $\beta = 0.2$ , indicating that the number of escaping points is low. As  $\beta$  is increased, this feature becomes less prominent. Additionally, the sets converge towards the classical Mandelbrot set for the 2nd-degree polynomial as  $\beta$  increases. The classical Mandelbrot set (Fig. 2(b)) and the generated Mandelbrot set for  $\beta = 1$  in Fig. 6(d) are almost similar.

In the second example, we consider  $A = [-1.5, 1.5]^2$ , K = 50, the color map presented in Fig. 1, and the following functions:

$$F_3(z) = z^8 + 1.08z + r, (21)$$

$$F_4(z) = z^8 - 0.05z + r. (22)$$

In Fig. 7, the Mandelbrot sets are generated for the polynomials  $F_3$ ,  $F_4$  by the Picard iteration. There is a 7-fold symmetry in both figures. From the figures, it is quite



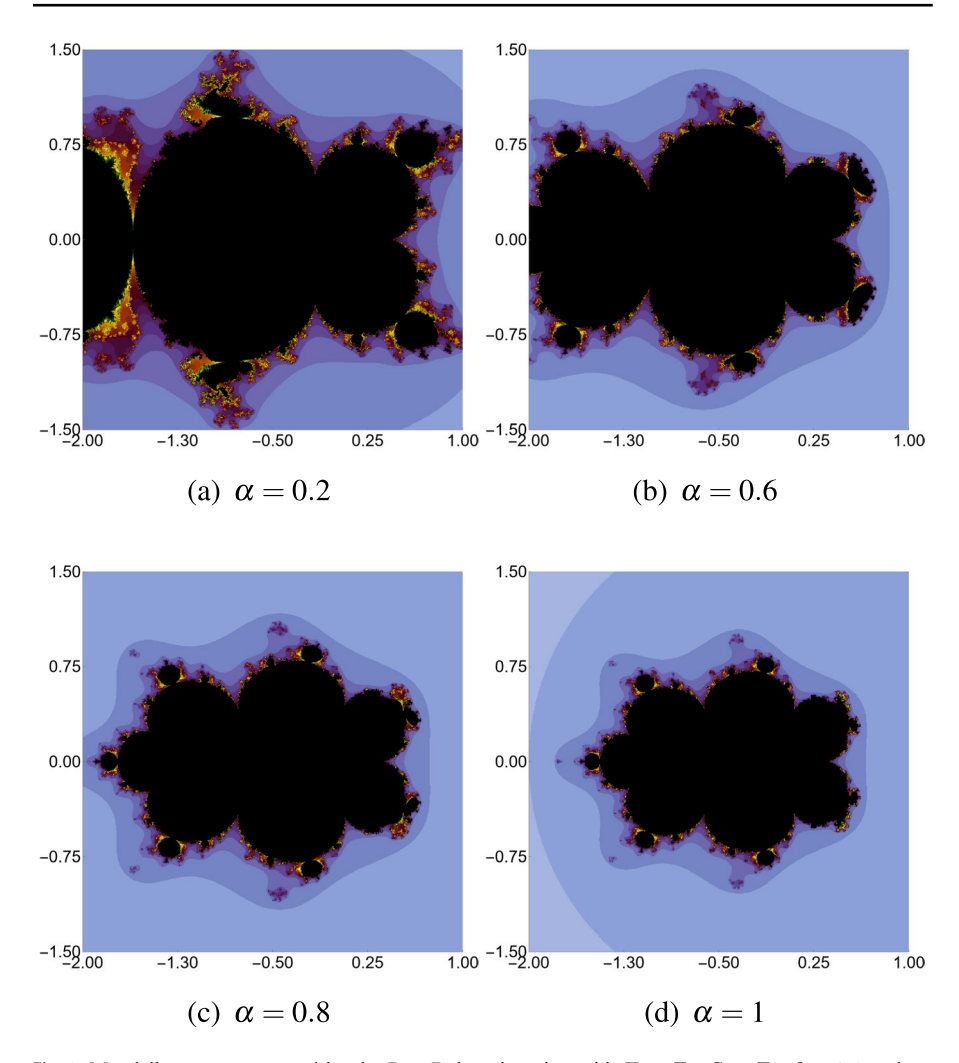


Fig. 3 Mandelbrot sets generated by the Das–Debata iteration with  $T=F_1,\,S=F_2,\,\beta=0.9$  and different values of  $\alpha$ 

interesting to note that only a little change in the coefficient of z in the polynomials impacts the size and shape of the sets.

In the Das-Debata iteration, we combine two 8th-degree polynomials  $T=F_3$  and  $S=F_4$ . The resulting Mandelbrot sets, which vary in the parameter  $\alpha$  and have a fixed value of  $\beta=0.08$ , are shown in Fig. 8. For  $\alpha=0.1$  in Fig. 8(a), the fractal appears connected with sharp filament-like protrusions extending outward from the center. Each of the seven primary components sharpens when  $\alpha$  increases, giving the sets a flower-like appearance. However, it is apparent that for  $\alpha=0.7$  and 1 in Figs. 8(c) and 8(d), there is little change in the structures of the sets, indicating that the variation of the parameter  $\alpha$  does not affect the overall structure of the sets. Despite this, the generated patterns in the Mandelbrot sets have striking differences



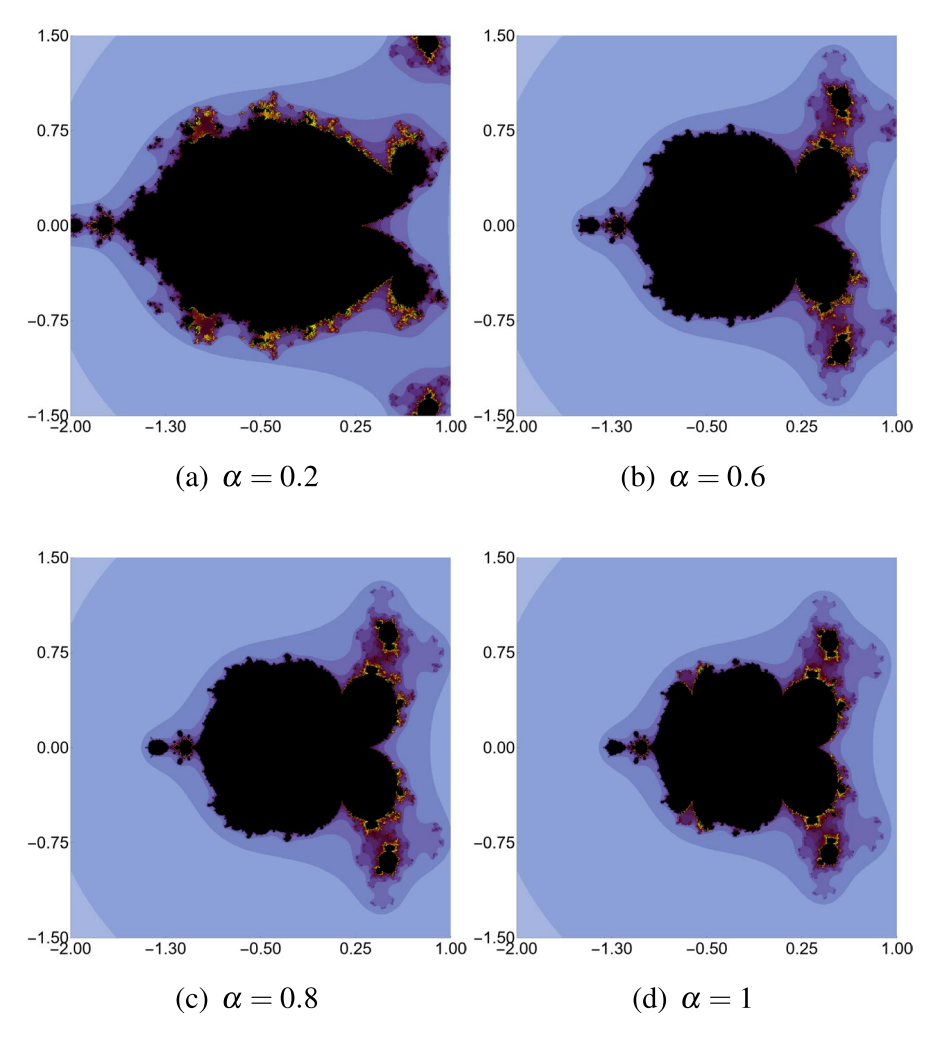


Fig. 4 Mandelbrot sets generated by the Das–Debata iteration with  $T=F_2,\,S=F_1,\,\beta=0.9$  and different values of  $\alpha$ 

in shape, size, and colors from those obtained by the Picard iteration. The Mandelbrot sets shown in Fig. 9 are generated with the same  $\alpha$  and  $\beta$  values as in Fig. 8, but with  $T=F_4$ ,  $S=F_3$ . The sets exhibit distinct patterns from those in Fig. 8. For  $\alpha=0.1$ , Fig. 9(a) shows seven identical petal-like components extending from the central core, with a bud-like structure on top of each of the seven components. The overall size of the sets decreases when  $\alpha$  is increased, and there are also some discernible changes in the structure of the seven primary components. Additionally, the bud-like structure began to move out from the main body as  $\alpha$  is increased. In contrast to the last illustration, the Mandelbrot sets do not appear to vary in color in the present one.

The Mandelbrot sets in Fig. 10 are obtained by varying the parameter  $\beta$  with fixed  $\alpha = 0.08$  and  $T = F_3$ ,  $S = F_4$ . The Mandelbrot set for  $\beta = 0.1$  is almost identical to



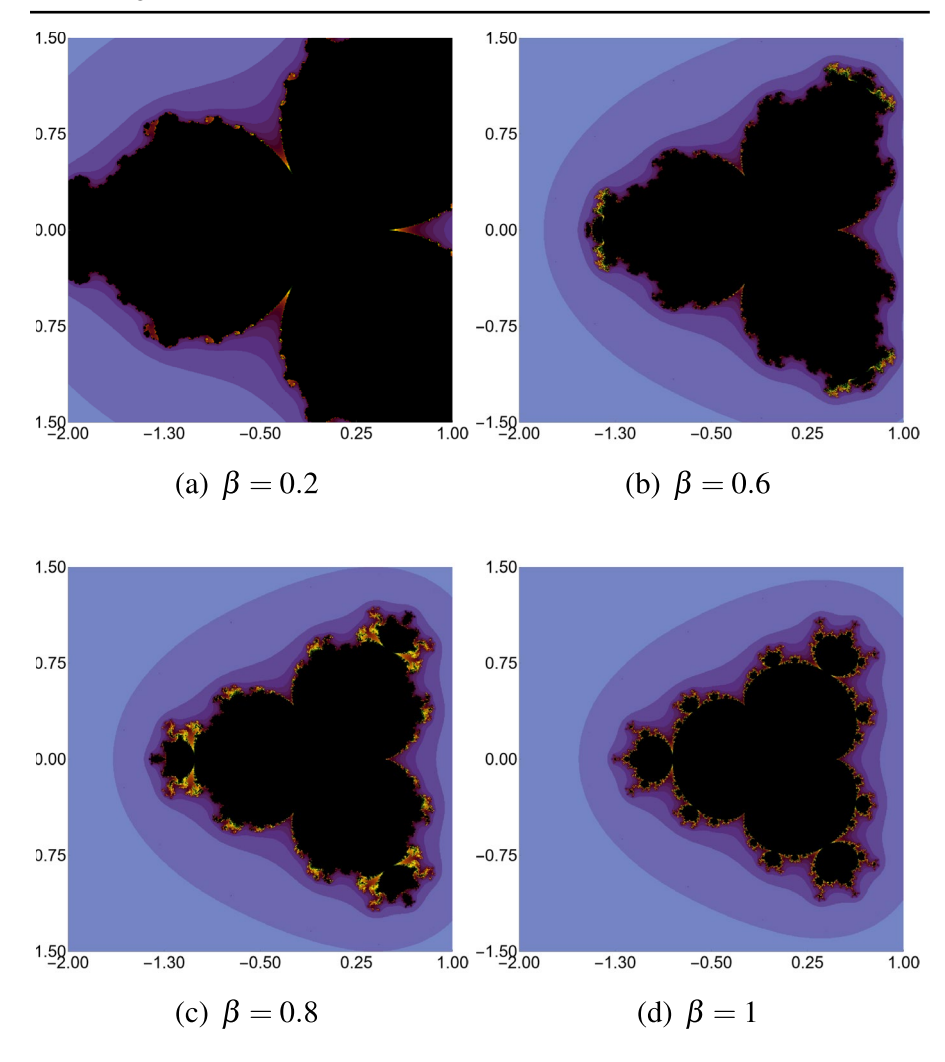


Fig. 5 Mandelbrot sets generated by the Das–Debata iteration with  $T=F_1,\,S=F_2,\,\alpha=0.01$  and different values of  $\beta$ 

that in Fig. 8(a) for  $\alpha=0.1$ . But the patterns are very different when  $\beta$  is increased. The size of the set drastically decreases when  $\beta$  is increased from 0.1 to 0.4. As the structure becomes increasingly fractured, the arm of the set exhibits more gaps and noticeable bulbous features for  $\beta=0.4$  and 0.7. The outer border displays a more noticeable petal-like structure at  $\beta=1$ , with the arms seeming smoother and the detailed filaments losing their dominance. Figure 11 displays the Mandelbrot sets that are generated by yet again altering the orders of the polynomials. Figures 11(a) and 11(b) which are obtained for  $\beta=0.1$  and 0.4 are almost identical with the sets generated for  $\alpha=0.1$  and 0.4 in Fig. 9. The arms of the Mandelbrot set grow increasingly fractured, and small satellite-like structures begin to emerge close to the border for



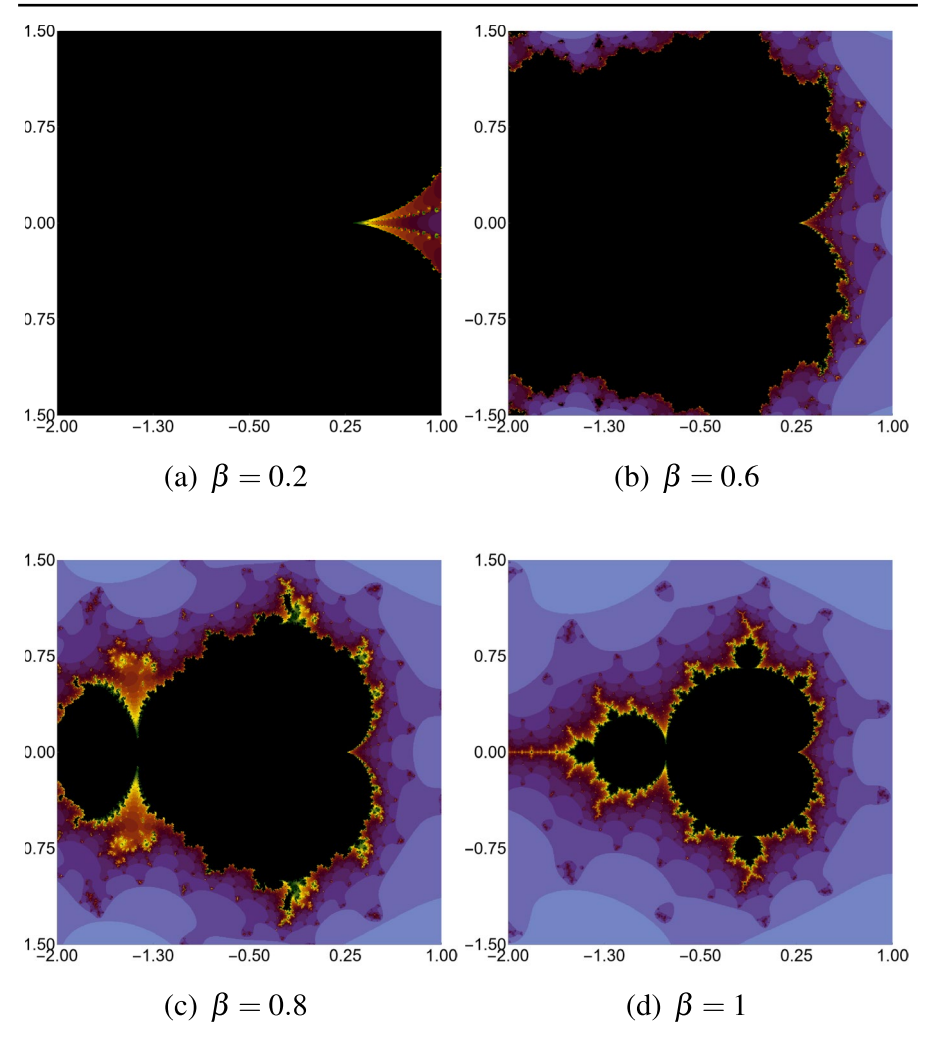


Fig. 6 Mandelbrot sets generated by the Das–Debata iteration with  $T=F_2,\,S=F_1,\,\alpha=0.01$  and different values of  $\beta$ 

 $\beta=0.7$ . The structure shows more fragmentation at  $\beta=1$ . There is some variation in color in the boundaries of the set only for the values  $\beta=0.7$  and 1.

In the third example, we consider  $A = [-1.5, 1.5]^2$ , K = 50, the color map presented in Fig. 1, and the following functions:

$$F_5(z) = z^8 + z + r, (23)$$

$$F_6(z) = z^5 + z + r. (24)$$

Mandelbrot sets produced by the Picard iteration for the 8th and 5th-degree polynomials,  $F_5$  and  $F_6$ , respectively, are shown in Fig. 12. Both sets are quite tiny and



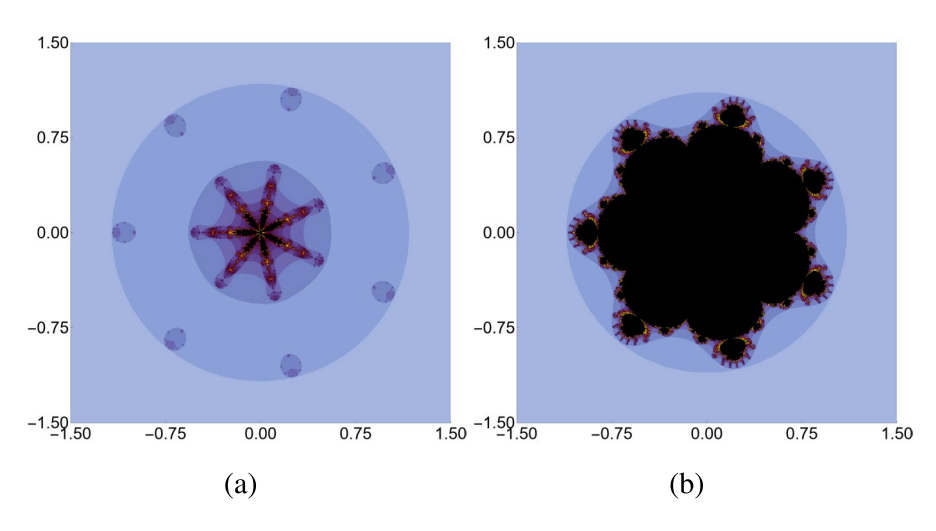


Fig. 7 Mandelbrot sets generated by Picard iteration with (a)  $F_3$  and (b)  $F_4$  functions

concentrated in the region's center. The image exhibits 7-fold symmetry for the 8th-degree polynomial and 4-fold symmetry for the 5th-degree polynomial.

In the Das–Debata iteration, we combine  $T = F_5$  and  $S = F_6$ . The resulting Mandelbrot sets, by varying the parameter  $\alpha$  with a fixed value of  $\beta = 0.01$ , are shown in Fig. 13. The figures suggest that both polynomials have an impact on the structure of the Mandelbrot sets. In Fig. 13(a), the figure is expanded to all regions with an irregular symmetry for  $\alpha = 0.1$ . The set's size drastically shrinks, and the shape nearly takes on a quadrilateral shape when  $\alpha$  is increased to 0.4. While the overall shape of the sets stays the same, there is a distinct drop in size as  $\alpha$  is increased more. The Mandelbrot sets with the same parameter values and shifting the orders of the polynomials, i.e.,  $T = F_5$ ,  $S = F_5$  in the Das-Debata iteration are shown in Fig. 14. The dark area in Fig. 14(a) expands outward and covers a larger area for  $\alpha = 0.1$ . There are structures that resemble petals, although they are irregular and not welldefined. In Fig. 14(b), when  $\alpha$  is increased to 0.4, the set seems more centered and more organized, with a distinct boundary and a little contraction in size. Also, the petal-like features become more uniformly spaced and sharper. The size of the sets progressively shrinks and the petal-like structures become more stable as the values of  $\alpha$  are increased to 0.7 and 1.

Figure 15 shows the Mandelbrot sets that combine the same 8th and 5th-degree polynomials  $T=F_5$ ,  $S=F_6$  in the Das–Debata iteration and vary the parameter  $\beta$  with a fixed value of  $\alpha=0.01$ . Figure 15(a) shows that the set has elongated, star-like shapes with sharp spikes for  $\beta=0.1$ . The black area is larger and takes up a significant amount of the area under consideration. The set's structure grows increasingly complex at  $\beta=0.4$ , with fractal-like patterns appearing in the arms. The star-like arms get more complex and exhibit greater self-similarity as the set shrinks a little, concentrating the complexity inward. The pattern becomes more balanced for  $\beta=0.7$ . The arms fold into a more rounded shape, and the core structure gets denser. With the same values of the parameters, the Mandelbrot sets obtained by chang-



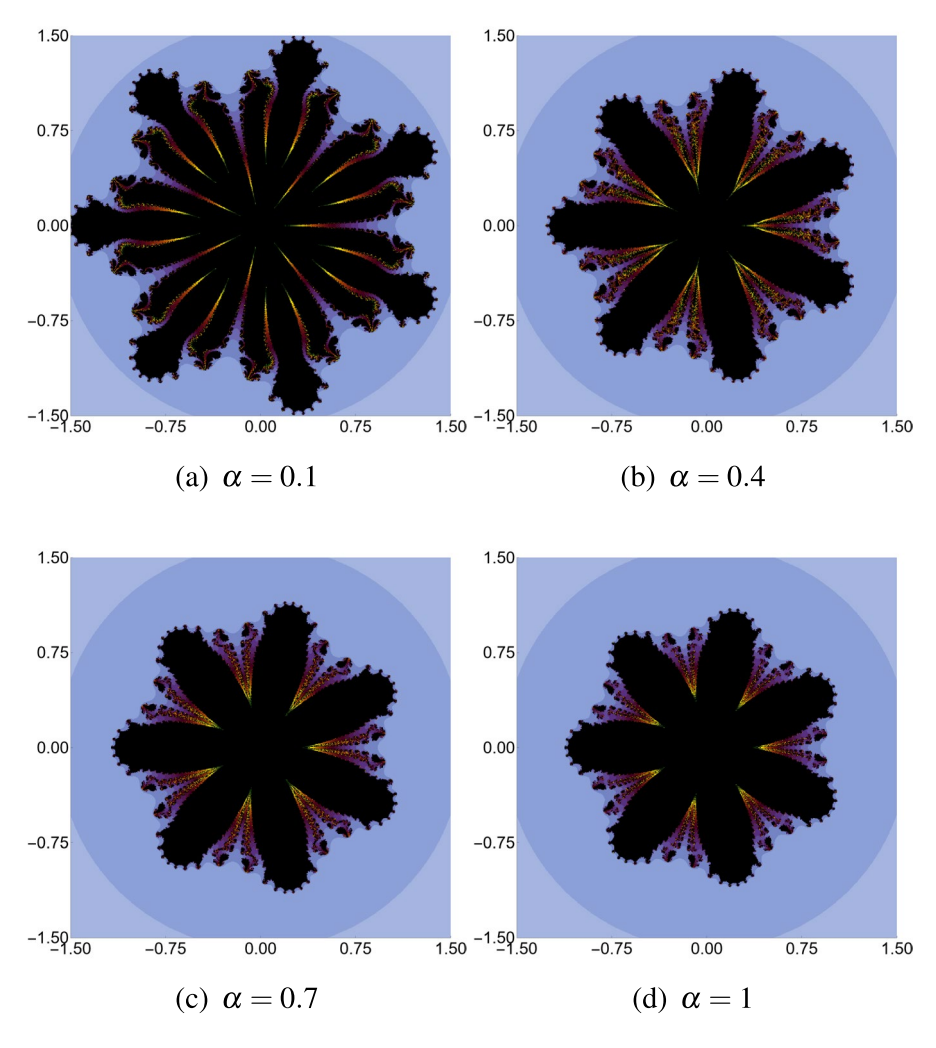


Fig. 8 Mandelbrot sets generated by the Das–Debata iteration with  $T=F_3,\,S=F_4,\,\beta=0.08$  and different values of  $\alpha$ 

ing the orders of the polynomials, i.e.,  $T=F_6$ ,  $S=F_5$ , are presented in Fig. 16. For  $\beta=0.1$  the dark area is wide, with extended arms reaching outward. The edges acquire more curvature and the lobes get more compact in the Mandelbrot set for  $\beta=0.4$ . The structure gets more regular as the fractal's overall size decreases, focusing the details inward. The sets contract more when the values of  $\beta$  are increased to 0.7 and 1, and the boundary features become more complex.



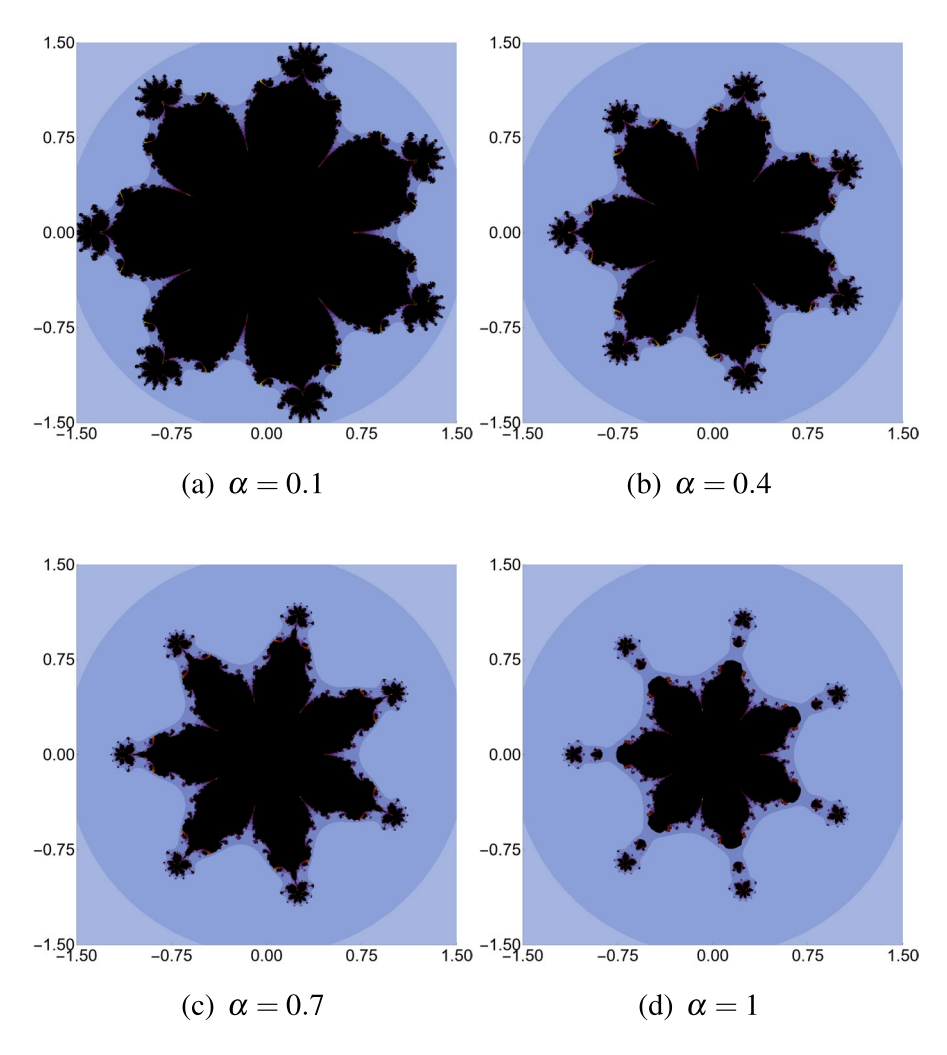


Fig. 9 Mandelbrot sets generated by the Das–Debata iteration with  $T=F_4,\,S=F_3,\,\beta=0.08$  and different values of  $\alpha$ 

## 5 Numerical results

When two distinct polynomials are used in the Das–Debata iteration for the generation process, the graphical examples of the Mandelbrot set from Section 4 exhibit complicated structures. As we can see from the graphical representations, the iteration parameters  $\alpha$ ,  $\beta$  have a significant impact on determining the size and shape of the Mandelbrot sets. It is quite interesting to study the dependency of the shape and size of the sets on the iteration parameters. We employ two numerical measures that track the escaping and non-escaping points separately, which were first presented in [17]. The first metric is the average escape time (AET), which tells us how many iterations on average were performed for the escaping points in a given area.



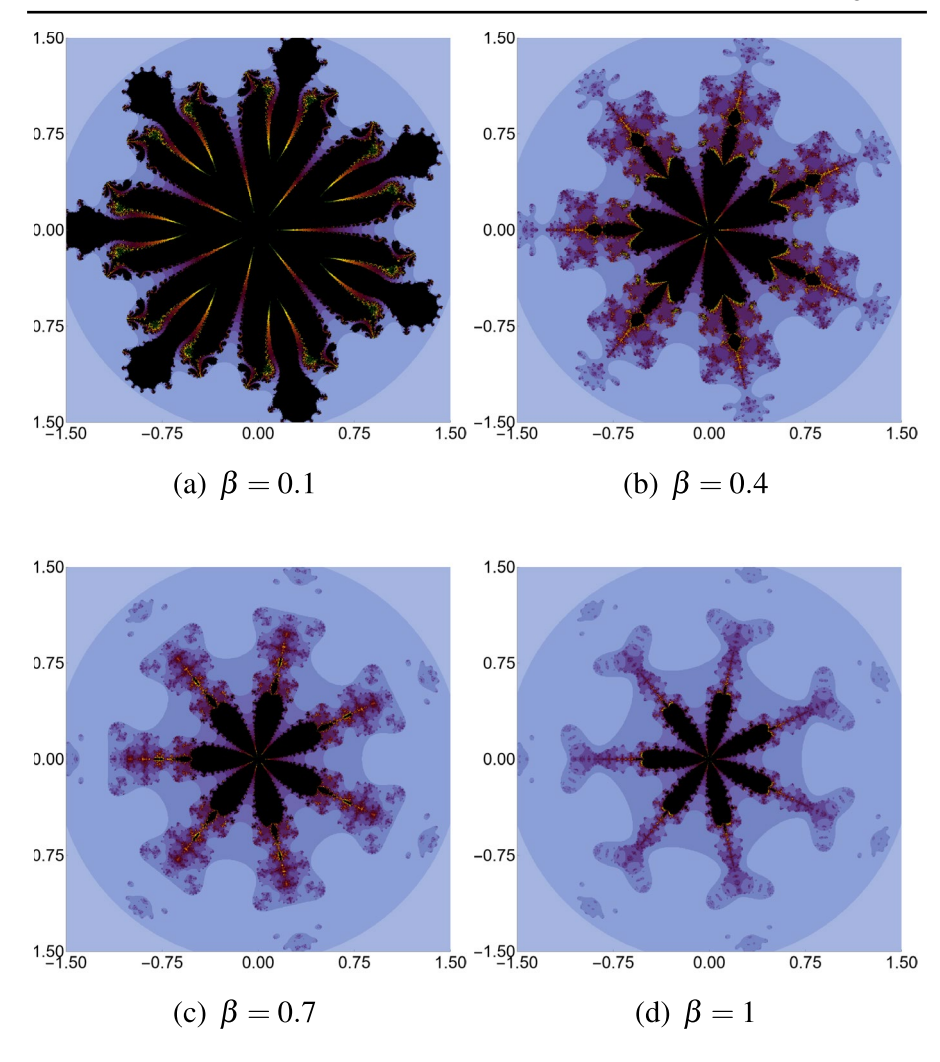


Fig. 10 Mandelbrot sets generated by the Das–Debata iteration with  $T=F_3,\,S=F_4,\,\alpha=0.08$  and different values of  $\beta$ 

Another important metric is the non-escaping area index (NAI), which provides us with insight into the relative set size in a specific area. It is defined as the ratio of the number of non-escaping points to the number of all points in the considered area.

In this study, the region A has been divided into an  $800 \times 800$  grid, and the parameters  $\alpha, \beta$  have been varied with a 0.01 step length. As a result, 10,000 images of the Mandelbrot set were generated for a single heatmap.

The AET and NAI plots for the Mandelbrot sets derived by merging the 4th and 2nd degree polynomials  $F_1$  and  $F_2$  in the Das-Debata iteration are displayed in Figs. 17 and 18, respectively. An early escape for the escaping points is shown by the blue area nearly everywhere in the parameter space of the AET plot in Fig. 17(a), which shows a homogeneous distribution in the AET values that is close to 5 in most places. When



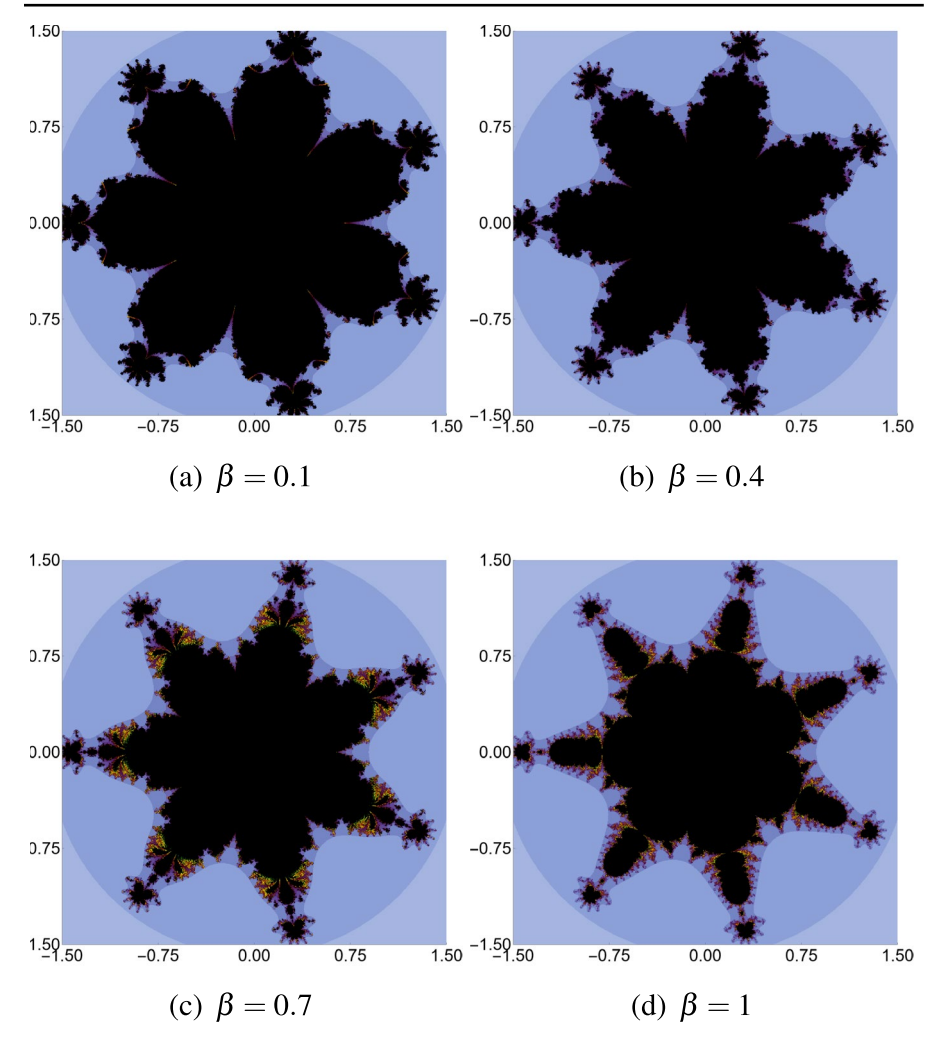


Fig. 11 Mandelbrot sets generated by the Das–Debata iteration with  $T=F_4,\,S=F_3,\,\alpha=0.08$  and different values of  $\beta$ 

the value of the parameter  $\beta$  is low, the AET values are greater. The AET values of 23.17 and 1.29 are the highest and lowest, respectively, at  $(\alpha, \beta) = (0.09, 0.01)$  and  $(\alpha, \beta) = (1, 0.53)$ . The AET plot in Fig. 17(b) displays nearly identical behavior as in the preceding instance, but with greater AET values, when the ordering of the polynomials is changed in the iteration process. In the majority of the parameter space, the AET values are near 10. However, a characteristic that stands out is that no points have left the region for the lower values of the parameters where the AET is not computed. In this case,  $(\alpha, \beta) = (0.05, 0.01)$  yields the greatest AET value 48.61, while  $(\alpha, \beta) = (0.96, 1)$  yields the lowest, 1.96. There are several very noticeable characteristics in the NAI plots from Fig. 18. The NAI value never reaches 1 in Fig. 18(a), indicating that there are always some escape spots in the area for all parameter values



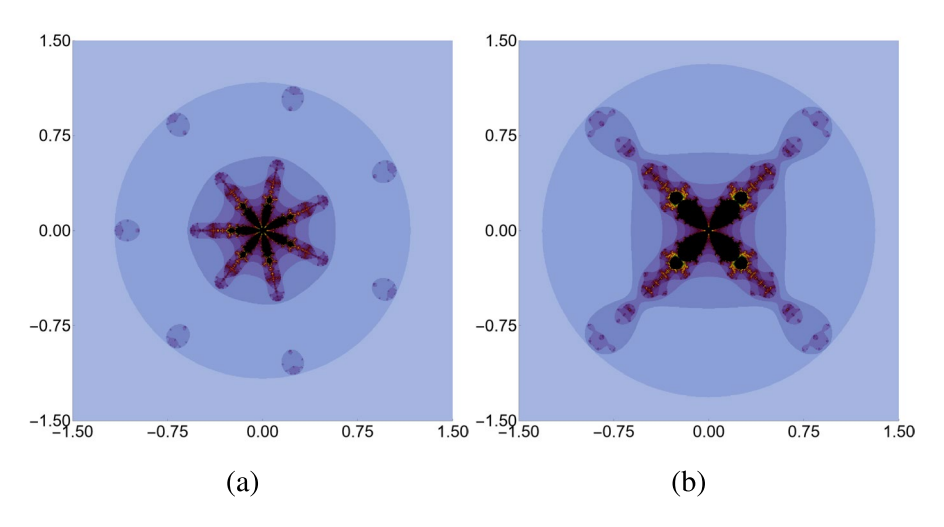


Fig. 12 Mandelbrot sets generated by Picard iteration with (a)  $F_5$  and (b)  $F_6$ 

taken into consideration. Higher NAI values are often obtained when the parameter  $\beta$  has a lower value and in the bottom half of the parameter space. When the NAI is 0.99 at  $(\alpha, \beta) = (0.14, 0.01)$ , the Mandelbrot set in this case takes up 99% of the whole area, while the smallest set is generated at  $(\alpha, \beta) = (0.01, 1)$ , where the NAI is 0.22. There are certain locations in the parameter space where both parameters take lower values, the NAI takes the maximum value of 1, and there are no escaping points in the area when the ordering of the polynomials is altered in the iteration, as seen in the NAI plot in Fig. 18(b). Also, compared to the previous case, the lower diagonal area of the parameter space is where the larger NAI values are obtained. The value of  $(\alpha, \beta) = (1, 1)$  yields the lowest NAI of 0.16.

Figures 19 and 20 displays the AET and NAI plots for the Mandelbrot sets created by combining the two 8th-degree polynomials  $F_3$  and  $F_4$  and altering the ordering of the polynomials in the Das–Debata iteration. In both cases, the AET plots (Fig. 19) show that the AET values are relatively low, indicating that the escaping points exit the region early in the iteration over the parameter space. Both scenarios have a similar pattern for the AET values, meaning that they increase as we approach lower values of the parameters  $\alpha$ ,  $\beta$ . The values of the parameter where a comparatively larger value of AET is obtained are shown in the red area of the figures. The maximum and minimum AET values for the former case are 4.24 and 0.6, respectively, at  $(\alpha, \beta) = (0.01, 0.28)$  and (0.95, 1). The minimum AET value for the latter case is 0.52 at  $(\alpha, \beta) = (1, 0.66)$  and maximum of 2.52 at  $(\alpha, \beta) = (0.03, 0.69)$ . For both cases, the higher NAI values are observed at the lower left corner of the parameter space where both  $\alpha$  and  $\beta$  have lower values. However, their variation in the whole parameter space is distinct, as can be seen from plots in Fig. 20. The NAI values in Fig. 20(a) steadily decline as  $\alpha$  increases, changing from red to green and finally blue. The decline in NAI values becomes more apparent as  $\beta$  increases, with deep blue shades dominating in the upper-right area. In contrast, the transition from high to low values seems smoother in Fig. 20(b), with a steadier decline from bottom to top



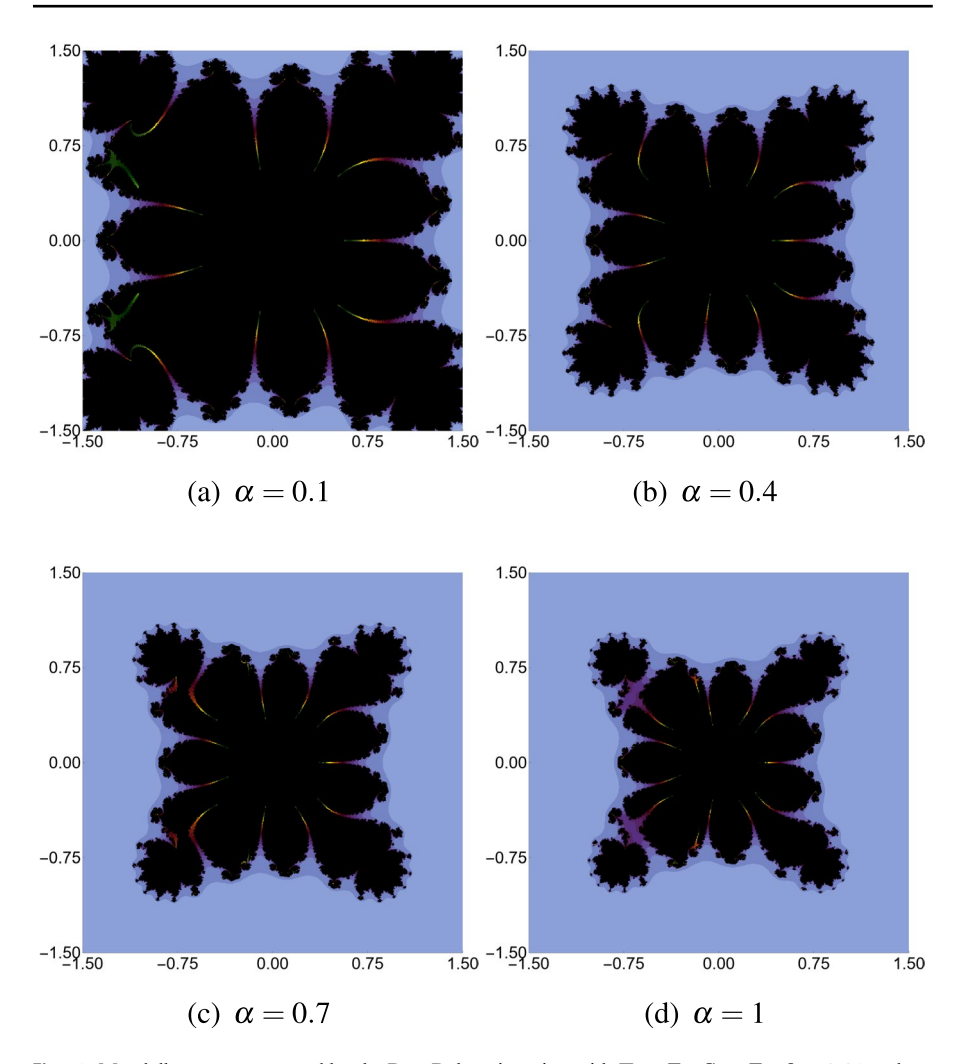


Fig. 13 Mandelbrot sets generated by the Das–Debata iteration with  $T=F_5, S=F_6, \beta=0.01$  and different values of  $\alpha$ 

and left to right in the parameter space. For the first case, the largest Mandelbrot set is generated at  $(\alpha, \beta) = (0.01, 0.01)$ , where the NAI value is 0.85, and the smallest at  $(\alpha, \beta) = (0.01, 1)$ , where the NAI value is 0.06. The latter instance, on the other hand, has a minimum NAI value of 0.05 at  $(\alpha, \beta) = (1, 1)$  and a maximum of 0.852 at  $(\alpha, \beta) = (0.01, 0.01)$ .

For the last example, we present the AET and NAI graphs for the Mandelbrot sets that are generated by combining the 8th and 5th-degree polynomials  $F_5$  and  $F_6$ , as well as by shifting their orderings in the Das-Debata iteration, in Figs. 21 and 22. The higher values of the AET, which are represented by the red-shaded area in the parameter space, are concentrated in the lower left corner at the lower values of the parameters in both Figs. 21(a) and 21(b). For the former case, as  $\alpha$ ,  $\beta$  increase, the



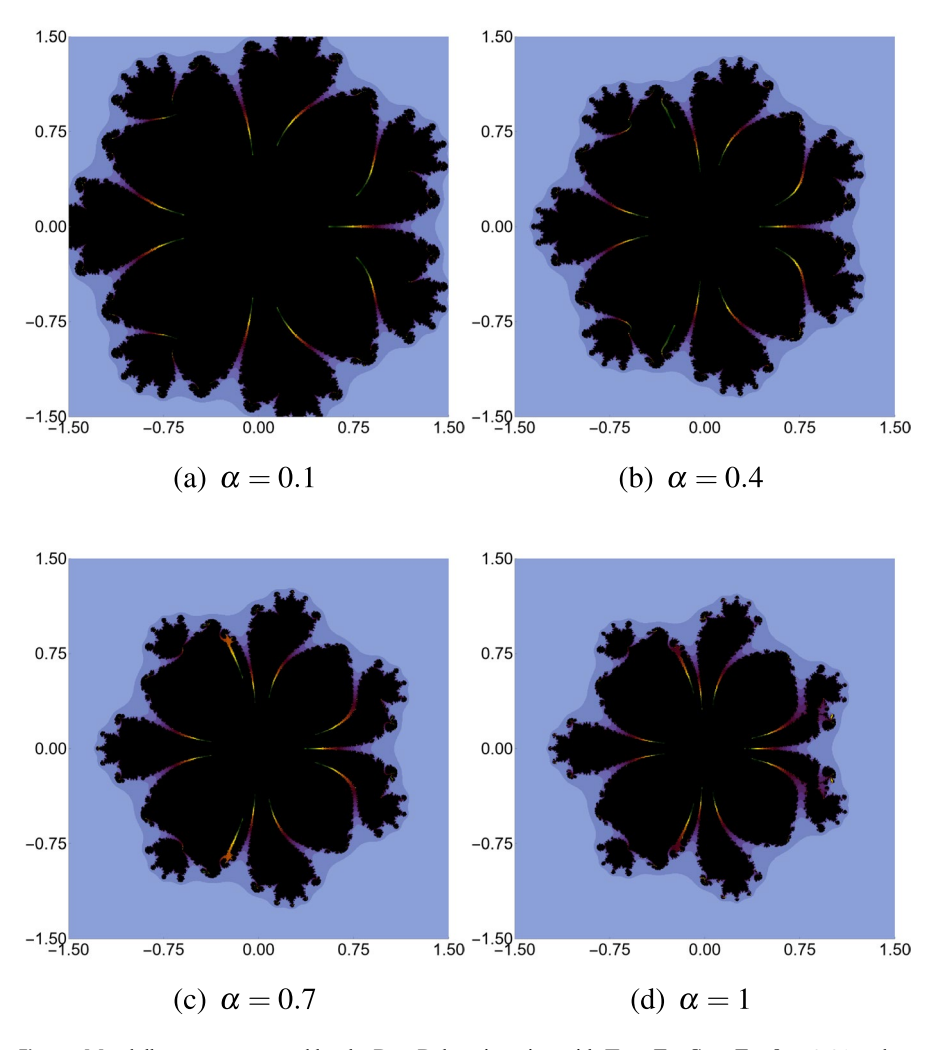


Fig. 14 Mandelbrot sets generated by the Das–Debata iteration with  $T=F_6, S=F_5, \beta=0.01$  and different values of  $\alpha$ 

AET values decrease, transitioning from yellow-green to deep blue in the upper-right region. Also, a noticeable gradient exists along both axes, with a relatively sharp transition from high to low values. The higher AET values are again found in the bottom-left section of Fig. 21(b), but they are not as noticeable as they were in the earlier case. Most parts of the plot are dominated by lower AET values, which are represented by blue shades, and the shift from high to low values seems smoother. The various color bar ranges in this figure show that the overall AET values are lower than in the previous plot. For the first plot, the maximum AET value is 4.88, while the lowest is 0.75 at  $(\alpha, \beta) = (0.02, 0.01)$  and (1, 1), respectively. The latter plot, however, has the greatest and lowest AET values at  $(\alpha, \beta) = (0.01, 0.01)$  and (1, 1), respectively, 6.39 and 0.75. In the case of NAI, both the plots in Fig. 22 show that



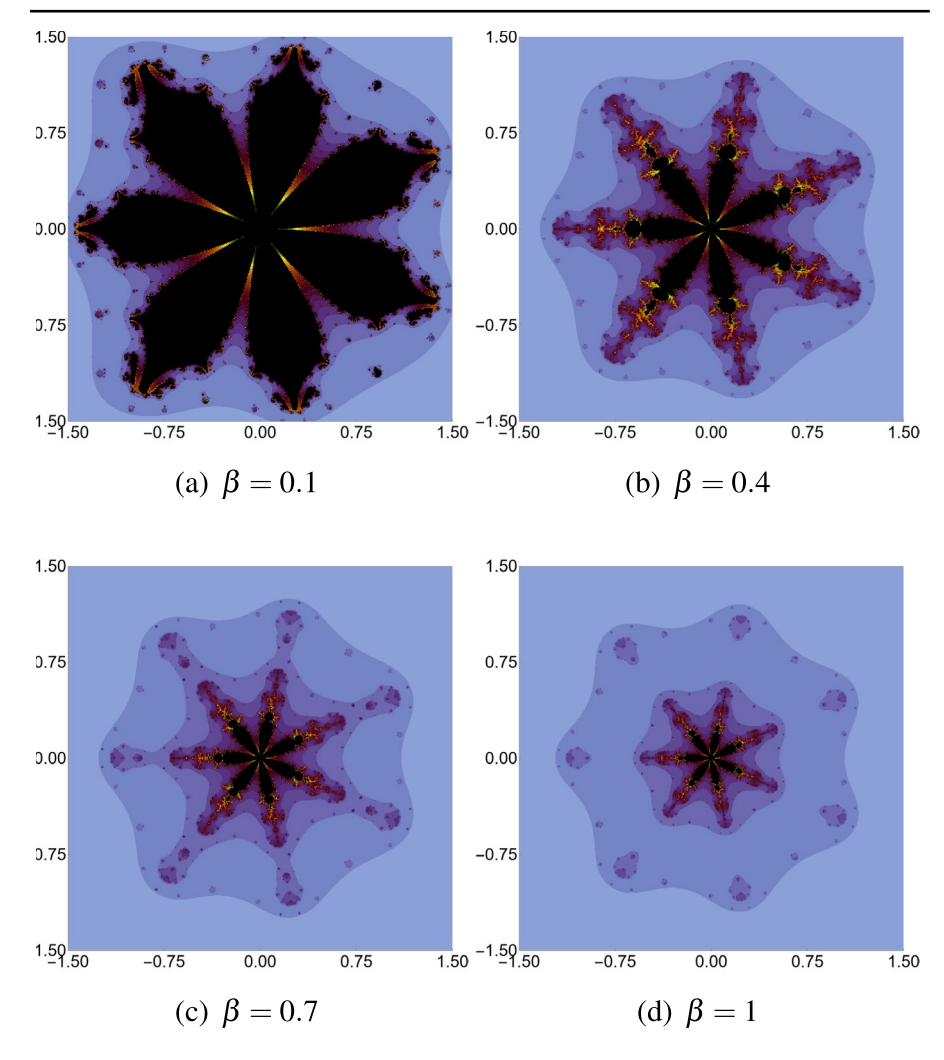


Fig. 15 Mandelbrot sets generated by the Das–Debata iteration with  $T=F_5, S=F_6, \alpha=0.01$  and different values of  $\beta$ 

the higher values represented by the red-shaded region in the parameter space are achieved at the lower left corner. Regarding NAI, both plots in Fig. 22 demonstrate that the lower left corner of the parameter space is where the higher values shown by the red-shaded region are attained. According to Fig. 22(a), the NAI values progressively drop as  $\alpha$  increases, changing from red to green and finally blue. Deep blue hues predominate in the top area, and the decline in NAI values becomes more apparent as  $\beta$  increases. In contrast to the first figure, the second scenario shows a more gradual change from red to blue and a smoother transition from high to low values. The second plot shows a more consistent gradient throughout the domain, but the general pattern is still the same. The parameters  $(\alpha, \beta) = (0.02, 0.01)$  and (1, 1) yield the greatest and smallest sets for the first case, respectively, with NAI values of 0.9



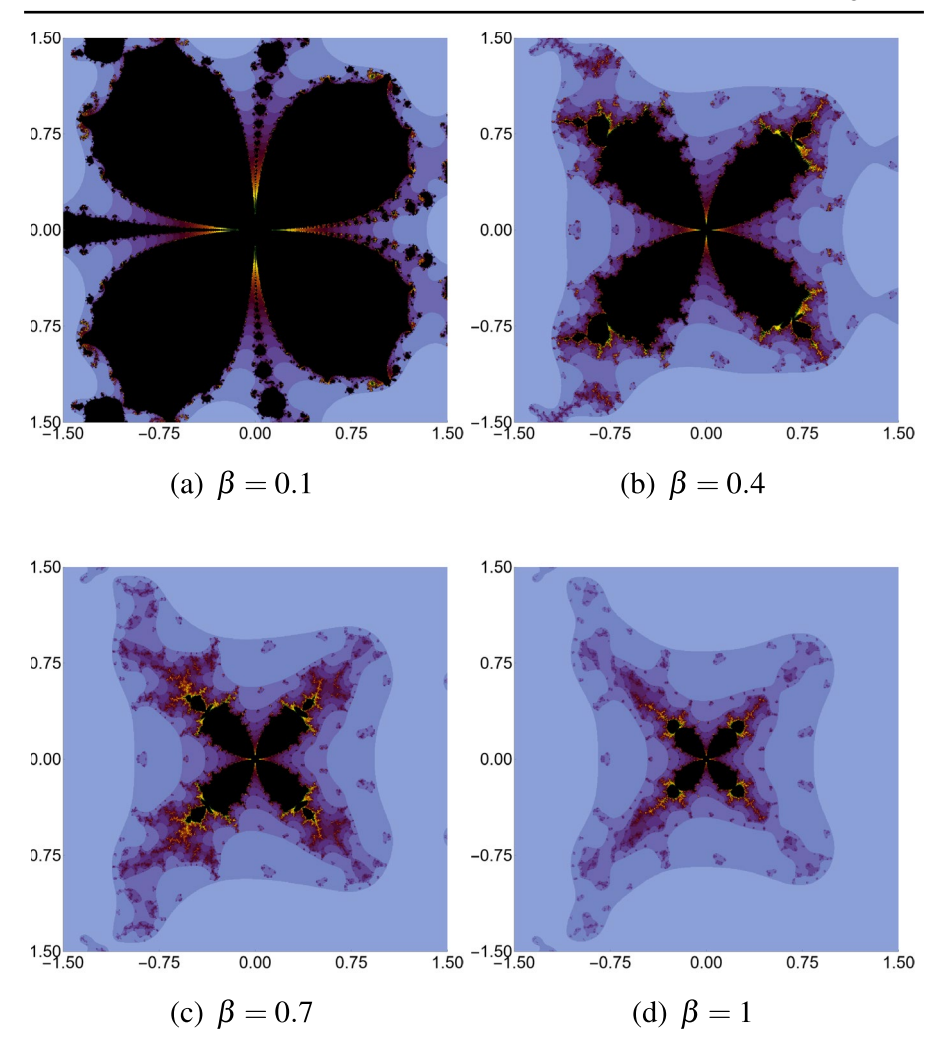


Fig. 16 Mandelbrot sets generated by the Das–Debata iteration with  $T=F_6, S=F_5, \alpha=0.01$  and different values of  $\beta$ 

and 0.004. The greatest and lowest NAI values for the latter case are 0.9 and 0.005 at  $(\alpha,\beta)=(0.01,0.01)$  and (1, 1), respectively. According to both graphs, greater NAI values are correlated with smaller  $\alpha$  and  $\beta$ , and these values fall as these parameters increase. In contrast to the first plot, which exhibits greater fluctuations in some areas, the second plot displays a transition that is more evenly distributed.



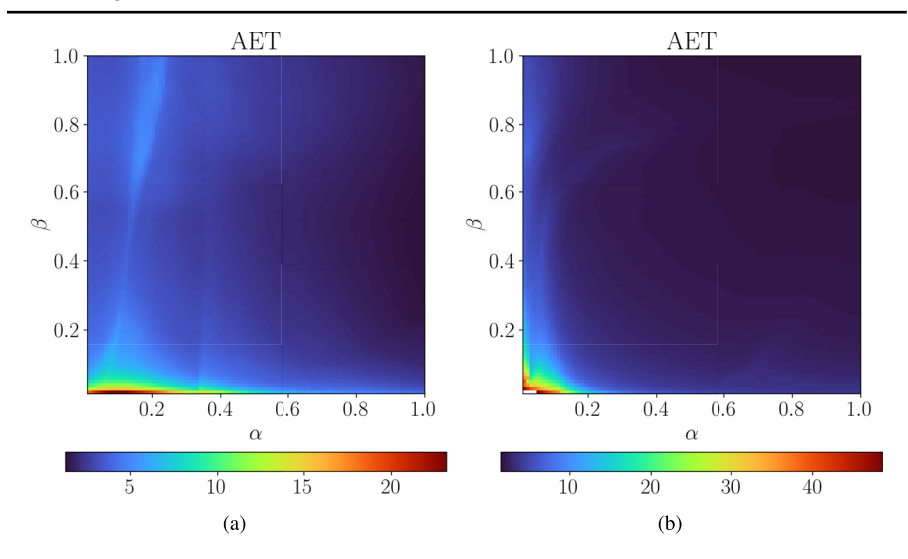


Fig. 17 AET plots for Mandelbrot sets obtained using Das–Debata iteration with (a)  $T=F_1, S=F_2$ , (b)  $T=F_2, S=F_1$ 

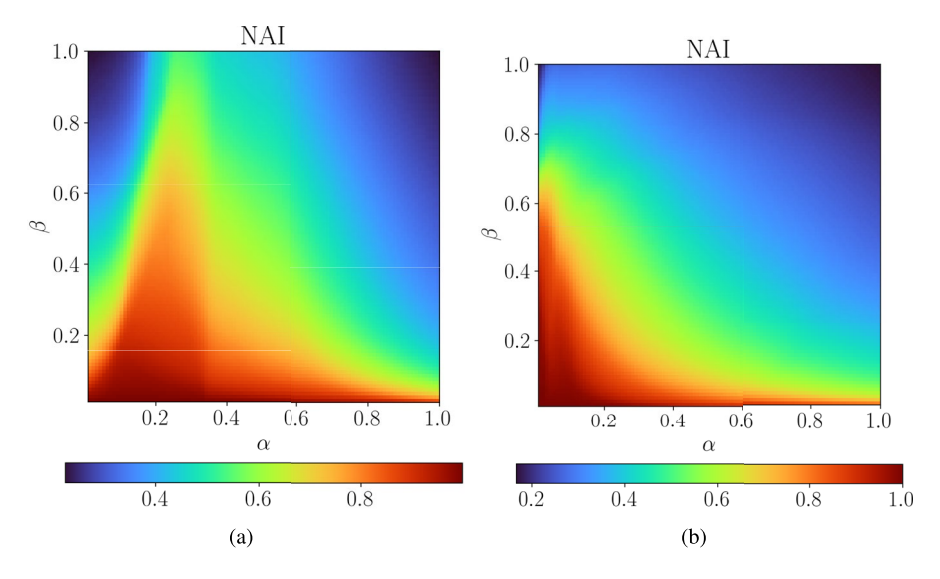


Fig. 18 NAI plots for Mandelbrot sets obtained using Das–Debata iteration with (a)  $T=F_1, S=F_2$ , (b)  $T=F_2, S=F_1$ 

## **6 Conclusions**

This study presented an approach to generating Mandelbrot sets using the escape time algorithm by iterating two distinct complex polynomial functions. We established escape criteria for the Das—Debata iterative method involving two distinct polynomials. Some interesting graphical representations of Mandelbrot sets are given, which



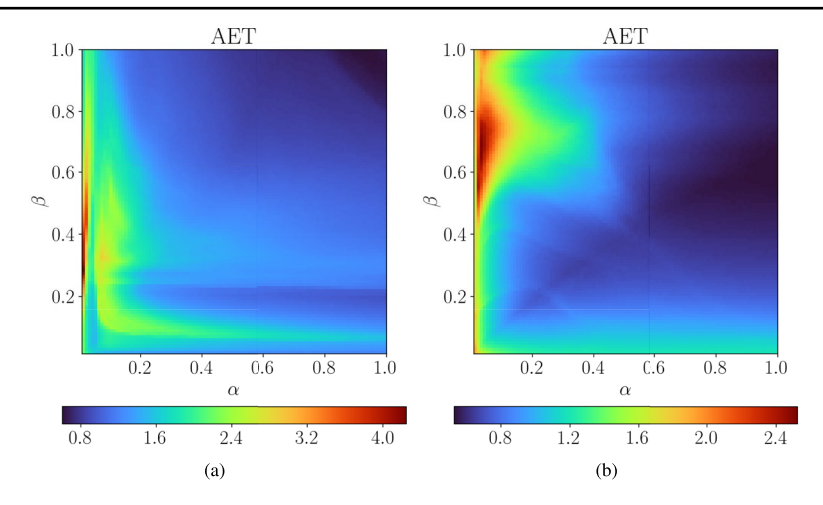


Fig. 19 AET plots for Mandelbrot sets obtained using Das–Debata iteration with (a)  $T=F_3, S=F_4$ , (b)  $T=F_4, S=F_3$ 

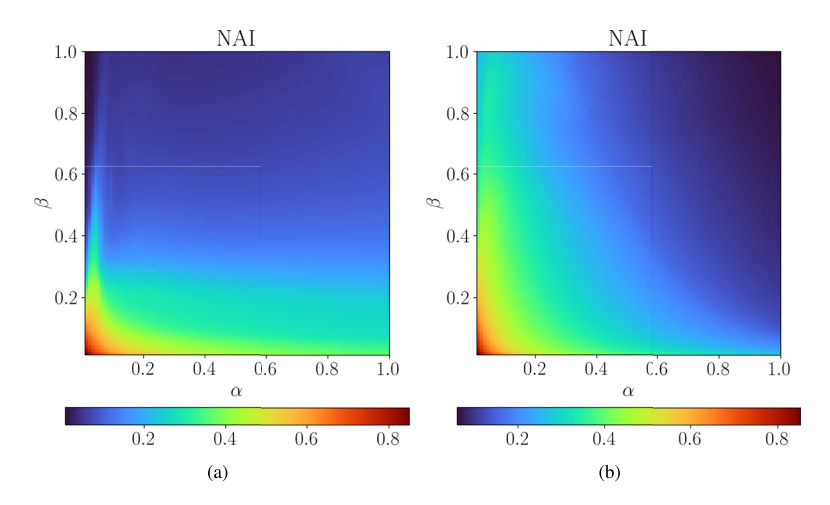


Fig. 20 NAI plots for Mandelbrot sets obtained using Das–Debata iteration with (a)  $T=F_3, S=F_4$ , (b)  $T=F_4, S=F_3$ 

reveal significant differences in their patterns when compared with the Mandelbrot sets generated with the Picard iteration. It has also been found that if we change the positions of the polynomials in the iteration process, the resultant Mandelbrot sets can have a different structure with the same parameter values. This showcases the utility of this method of merging multiple polynomials in a single iterative method to generate different fractal patterns. The fractal patterns created by this approach often has the influence of both the polynomials in their structures. For example, the Mandelbrot sets obtained by merging 2nd and 4th-degree polynomials can produce the classical Mandelbrot set as well as some other distinctive structures as we found



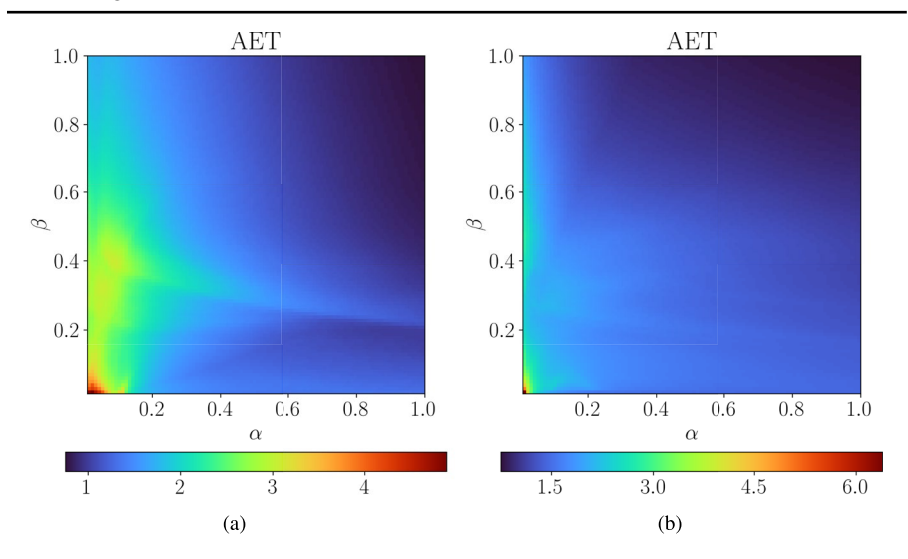


Fig. 21 AET plots for Mandelbrot sets obtained using Das–Debata iteration with (a)  $T=F_5, S=F_6$ , (b)  $T=F_6, S=F_5$ 

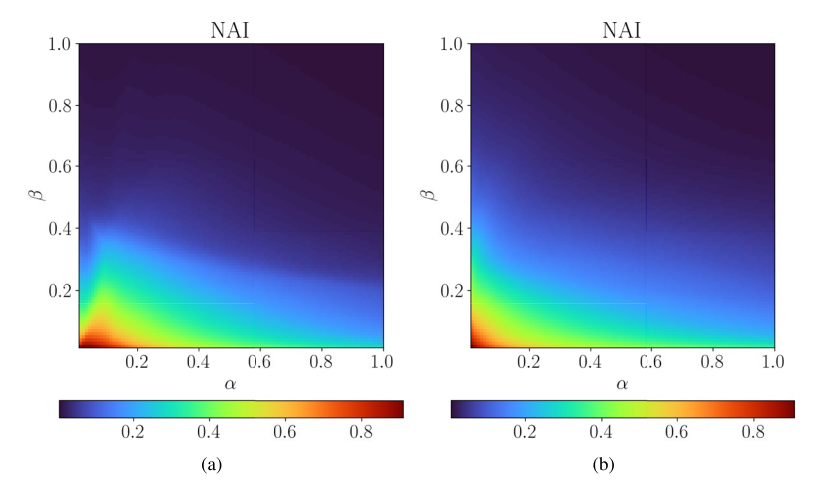


Fig. 22 NAI plots for Mandelbrot sets obtained using Das–Debata iteration with (a)  $T=F_5, S=F_6$ , (b)  $T=F_6, S=F_5$ 

in the graphical examples. Furthermore, our analysis of the numerical measures AET and NAI reveals a complex and nonlinear dependency on iteration parameters.

The concept of employing multiple operators in fixed-point iterations, which has been extensively explored in the literature, constitutes a powerful and flexible approach for fractal generation. This framework allows for the synthesis of complex dynamical behaviors by alternating or combining different operators within iterative schemes. Such an approach not only enriches the geometry of the resulting fractals but also broadens the analytical tools available for their study.



Future research may investigate the effects of alternative polynomial combinations, including higher-degree or asymmetric polynomials, and their influence on the stability and structure of the generated sets. Moreover, this methodology can be extended to encompass other classes of functions, such as exponential, hyperbolic, logarithmic, or trigonometric functions. These function classes, with their distinct dynamical characteristics, could produce qualitatively different fractal structures and may uncover new fixed-point behaviors or convergence patterns that are not apparent in purely polynomial contexts.

An additional direction for exploration involves applying this multi-operator iterative framework to the generation of Julia sets. Given the deep connections between Julia and Mandelbrot sets the adaptation of multi-function iterations to Julia set construction could provide further insight into their bifurcation landscapes and connectivity properties. Investigating how the interaction of multiple operators affects the local and global features of Julia sets could be particularly fruitful.

Furthermore, extending this methodology beyond the conventional complex plane to more generalized number systems offers another promising research direction. For example, using trinion numbers [5] or quaternion numbers [12] in place of complex numbers introduces higher-dimensional dynamics into the iteration process. These generalized algebras allow for the construction of fractal sets in three or four dimensions, opening new possibilities for visualization, analysis, and potential applications in fields such as physics, signal processing, and computer graphics. The extension of fixed-point iteration theory to these non-commutative or non-associative number systems poses significant mathematical challenges, but also presents an opportunity to deepen our understanding of fractal geometry in higher-dimensional spaces.

Author Contributions S.Roy: Conceptualization, Formal analysis, Investigation, Visualization, Writing - original draft, Writing - review & editing; K.Gdawiec: Conceptualization, Formal analysis, Methodology, Software, Supervision, Validation, Writing - review & editing

**Funding** This research received no external funding.

Data Availability The data that support the findings of this study are available from the corresponding author, upon reasonable request.

#### Declarations

**Competing Interests** The authors declare no competing interests.

**Open Access** This article is licensed under a Creative Commons Attribution-NonCommercial-NoDerivatives 4.0 International License, which permits any non-commercial use, sharing, distribution and reproduction in any medium or format, as long as you give appropriate credit to the original author(s) and the source, provide a link to the Creative Commons licence, and indicate if you modified the licensed material. You do not have permission under this licence to share adapted material derived from this article or parts of it. The images or other third party material in this article are included in the article's Creative Commons licence, unless indicated otherwise in a credit line to the material. If material is not included in the article's Creative Commons licence and your intended use is not permitted by statutory regulation or exceeds the permitted use, you will need to obtain permission directly from the copyright holder. To view a copy of this licence, visit <a href="https://creativecommons.org/licenses/by-nc-nd/4.0/">https://creativecommons.org/licenses/by-nc-nd/4.0/</a>.



## References

- 1. Adhikari, N., Sintunavarat, W.: Exploring the Julia and Mandelbrot sets of  $z^p + \log c^t$  using a four-step iteration scheme extended with s-convexity. Math. Comput. Simul. **220**, 357–381 (2024). https://doi.org/10.1016/j.matcom.2024.01.010
- 2. Adhikari, N., Sintunavarat, W.: The Julia and Mandelbrot sets for the function  $z^p qz^2 + rz + \sin c^w$  exhibit Mann and Picard-Mann orbits along with s-convexity. Chaos, Soliton. Fract. **181**, 114600 (2024). https://doi.org/10.1016/j.chaos.2024.114600
- Antal, S., Tomar, A., Prajapati, D., Sajid, M.: Variants of Julia and Mandelbrot sets as fractals via Jungck—Ishikawa fixed point iteration system with s-convexity. AIMS Math. 7(6), 10939–10957 (2022). https://doi.org/10.3934/math.2022611
- Ashish, Rani, M., Chugh, R.: Julia sets and Mandelbrot sets in Noor orbit. Appl. Math. Comput. 228, 615–631 (2014). https://doi.org/10.1016/j.amc.2013.11.077
- Atangana, A., Mekkaoui, T.: Trinition the complex number with two imaginary parts: Fractal, chaos and fractional calculus. Chaos, Soliton. Fract. 128, 366–381 (2019). https://doi.org/10.1016/j.chaos. 2019.08.018
- 6. Barnsley, M.: Fractals Everywhere, 2nd edn. Academic Press, Boston (1993)
- Beardon, A.: Iteration of rational functions: Complex analytic dynamical systems. Springer-Verlag, New York (1991)
- 8. Das, G., Debata, J.: Fixed points of quasinonexpansive mappings. Indian J. Pure Appl. Math. 17(11), 1263–1269 (1986)
- Devaney, R.: A First Course in Chaotic Dynamical Systems: Theory and Experiment, 2nd edn. CRC Press, Boca Raton (2020)
- Durkin, M.: Observations on the dynamics of the complex cosine-root family. J. Diff. Equation. Appl. 4(3), 215–228 (1998). https://doi.org/10.1080/10236199808808139
- 11. Gdawiec, K.: Fractal patterns from the dynamics of combined polynomial root finding methods. Nonlinear Dyna. 90(4), 2457–2479 (2017). https://doi.org/10.1007/s11071-017-3813-6
- Gdawiec, K., Fariello, R., Santos, Y.: On the quaternion Julia sets via Picard-Mann iteration. Nonlinear Dyna. 111(18), 17591–17603 (2023). https://doi.org/10.1007/s11071-023-08785-0
- Ishikawa, S.: Fixed points by a new iteration method. Proceed. American Math. Soc. 44(1), 147–150 (1974). https://doi.org/10.1090/S0002-9939-1974-0336469-5
- Kalantari, B.: Polynomial Root-Finding and Polynomiography. World Scientific, Singapore. (2009) https://doi.org/10.1142/6265
- 15. Keen, L., Kotus, J.: Dynamics of the family  $\lambda \tan z$ . Conformal Geomet. Dyna. 1, 28–57 (1997). h ttps://doi.org/10.1090/S1088-4173-97-00017-9
- Kumari, S., Gdawiec, K., Nandal, A., Kumar, N., Chugh, R.: An application of viscosity approximation type iterative method in the generation of Mandelbrot and Julia fractals. Aequationes Math. 97(2), 257–278 (2023). https://doi.org/10.1007/s00010-022-00908-z
- 17. Kumari, S., Gdawiec, K., Nandal, A., Kumar, N., Chugh, R.: On the viscosity approximation type iterative method and its non-linear behaviour in the generation of Mandelbrot and Julia sets. Numer. Algo. 96(1), 211–236 (2024). https://doi.org/10.1007/s11075-023-01644-4
- Kumari, S., Gdawiec, K., Nandal, A., Postolache, M., Chugh, R.: A novel approach to generate Mandelbrot sets, Julia sets and biomorphs via viscosity approximation method. Chaos, Soliton. Fract. 163, 112540 (2022). https://doi.org/10.1016/j.chaos.2022.112540
- 19. Lakhtakia, A., Varadan, V., Messier, R., Varadan, V.: On the symmetries of the Julia sets for the process  $z \to z^p + c$ . J. Phys. A: Math. General **20**(11), 3533 (1987). https://doi.org/10.1088/0305-4470/20/11/051
- 20. Li, D., Tanveer, M., Nazeer, W., Guo, X.: Boundaries of filled Julia sets in generalized Jungck-Mann orbit. IEEE Access 7, 76859–76867 (2019). https://doi.org/10.1109/ACCESS.2019.2920026
- 21. Mandelbrot, B.: The Fractal Geometry of Nature. W.H. Freeman and Company, San Francisco (1982)
- Nakamura, K.: Iterated inversion system: an algorithm for efficiently visualizing Kleinian groups and extending the possibilities of fractal art. J. Math. Arts 15(2), 106–136 (2021). https://doi.org/10.1080 /17513472.2021.1943998
- Rana, R., Chauhan, Y., Negi, A.: Non linear dynamics of Ishikawa iteration. Int. J. Comput. Appl. 7(13), 43–49 (2010). https://doi.org/10.5120/1320-1674
- Rani, M., Kumar, V.: Superior Julia sets. J. Korea Soc. Math. Educ. Series D: Res. Math. Educ. 8(4), 261–277 (2004)



- Rawat, S., Prajapati, D.J., Tomar, A., Gdawiec, K.: Generation of Mandelbrot and Julia sets for generalized rational maps using SP-iteration process equipped with s-convexity. Math. Comput. Simul. 220, 148–169 (2024). https://doi.org/10.1016/j.matcom.2023.12.040
- Roy, S., Gdawiec, K., Saha, P., Choudhury, B.: Exploring fractal geometry through Das–Debata iteration: A new perspective on Mandelbrot and Julia sets. Chaos, Soliton. Fract. 199(part 1), 116617 (2025). https://doi.org/10.1016/j.chaos.2025.116617
- Srivastava, R., Tassaddiq, A., Kasmani, R.: Escape criteria using hybrid Picard S-iteration leading to a comparative analysis of fractal Mandelbrot sets generated with S-iteration. Fractal. Fraction. 8(2), 116 (2024). https://doi.org/10.3390/fractalfract8020116
- 28. Tanveer, M., Gdawiec, K.: Application of CR iteration scheme in the generation of Mandelbrot sets of  $z^p + \log c^t$  function. Qualitat. Theory Dyna. Syst. **23**(1 supplement), 297 (2024). https://doi.org/10.1007/s12346-024-01160-3
- 29. Tanveer, M., Nazeer, W., Gdawiec, K.: On the Mandelbrot set of  $z^p + \log c^t$  via the Mann and Picard-Mann iterations. Math. Comput. Simul. **209**, 184–204 (2023). https://doi.org/10.1016/j.matcom.2023.02.012
- Tassaddiq, A.: General escape criteria for the generation of fractals in extended Jungck-Noor orbit. Math. Comput. Simul. 196, 1–14 (2022). https://doi.org/10.1016/j.matcom.2022.01.003
- Tassaddiq, A., Tanveer, M., Azhar, M., Lakhani, F., Nazeer, W., Afzal, Z.: Escape criterion for generating fractals using Picard-Thakur hybrid iteration. Alexandria Eng. J. 100(2), 331–339 (2024). https://doi.org/10.1016/j.aej.2024.03.074
- Xiangdong, L., Zhiliang, Z., Guangxing, W., Weiyong, Z.: Composed accelerated escape time algorithm to construct the general Mandelbrot set. Fractals 9(2), 149–153 (2001). https://doi.org/10.1142/S0218348X01000580

Publisher's Note Springer Nature remains neutral with regard to jurisdictional claims in published maps and institutional affiliations.

## **Authors and Affiliations**

# Subhadip Rov<sup>1</sup> · Krzysztof Gdawiec<sup>2</sup>

- Krzysztof Gdawiec krzysztof.gdawiec@us.edu.pl
   Subhadip Roy subhadip 123@yahoo.com
- Department of Mathematics, Indian Institute of Engineering Science and Technology, Shibpur, 711103 Howrah, India
- Institute of Computer Science, University of Silesia, Bedzinska 39, 41-200 Sosnowiec, Poland

